ACADEMIA ROMÂNĂ
Revue Roumaine de Chimie
http://web.icf.ro/rrch/

Rev. Roum. Chim.,
2011, *56*(10-11), 1003-1009

ELECTRODEPOSITION OF Ni-CERIA NANOCOMPOSITE COATINGS AND THEIR CORROSION BEHAVIOR

Nicoleta CIOATERĂ,[a] Adriana SAMIDE,[a*] Aurelia MAXUT,[a] Rose-Noëlle VANNIER[b] and Michel TRAISNEL[c]

[a] University of Craiova, Faculty of Chemistry, 107I Calea Bucureşti str., Craiova 200400, Roumania
[b] Ecole Nationale Supérieure de Chimie de Lille, Unité de Catalyse et de Chimie du Solide, UMR 8181 CNRS, 59652 Villeneuve d'Ascq, France
[c] Ecole Nationale Supérieure de Chimie de Lille (ENSCL), Unité Matériaux et Transformations (CNRS UMR 8207 – Université Lille 1), 59652 Villeneuve d'Ascq, France

Received June 3, 2010

Ni/CeO_2 composite coatings were electrochemically deposited from a Watts bath on carbon steel. Nanostructured ceria powder synthesized by Pechini method was co-deposited with nickel. The structure and morphology of CeO_2 powder were evidenced by X-ray diffraction (XRD), and scanning electron microscopy (SEM). Pure Ni deposits were also obtained under the same experimental conditions for comparison. The electrodeposition was carried out at room temperature. The influence of several deposition parameters such as current density, deposition time, and ceramic bath loading on the coating structure and morphology was investigated by XRD and SEM. In order to evaluate the effect of ceria insertion on the nickel corrosion resistance, pure Ni and Ni/CeO_2 composite coatings were further tested using potentiodynamic and electrochemical impedance spectroscopy measurements in 0.1 M HCl solution at room temperature. An improvement of nickel corrosion resistance after reinforcement with nanosized ceria was evidenced.

INTRODUCTION

A number of studies have reveled that ceria films can be used as corrosion protective coating for metals and alloys in aqueous media and in high temperature conditions.[1, 2] Rare-earth doped ceria exhibited higher ionic conductivities than zirconia-based ceramics which make them appropriate for applications in solid oxide fuel cells (SOFCs).[3] In addition to their electrical properties which recommend them as anodes and electrolytes, ceria-based thin films can prevent the degradation of electrolyte/electrode interface, as well as the corrosion of interconnectors. Metal matrix composites reinforced with rare earth oxides can find applications in the aerospace industry due to their high oxidation temperature.

Previous studies revealed that the nature and composition of composite components, as well as ceramic particle sizes strongly affect the metal matrix composite properties.[4, 5] Moreover, the uniform distribution of second-phase particles into metal matrix proved to be essential.

The presence of solid particles in nickel plating bath disturbs the growth of nickel crystals by inducing new nucleation sites. Thus, the finely crystalline coatings could be obtained, leading to an improvement of their anticorrosion properties.[6] Nevertheless, due to the disturbance of nickel matrix structure, the incorporation of ceramic particles may lead to the formation of cracks and pores as a result of internal stresses.

With the aim to investigate the effect of nanostructured ceria on the corrosion protective

* Corresponding author: samide_adriana@yahoo.com

properties of nickel coatings onto carbon steel substrate, pure Ni and Ni/CeO_2 composite coatings have been electrodeposited on a carbon steel plate. The protection efficiency against corrosion in 0.1 M HCl aqueous solution was evaluated from electrochemical measurements.

RESULTS AND DISCUSSION

Powder and coatings structure and morphology

XRD pattern of calcined ceria powder is shown in Fig. 1. Only the characteristic peaks of fluorite type crystal structure (space group $Fm\bar{3}m$) were evidenced. The crystallite size of the powder was calculated using the Scherrer equation: $D = \frac{0.9\lambda}{\beta\cos\theta}$, where D is the crystallite size, λ is the radiation wavelenght, β is the half-maximum peak width, and θ is the angular position. A value of 11 nm was thus obtained.

The nanosized nature of the powder was also evidenced by SEM. The typical powder morphology is shown in Fig. 2.

Fig. 3 shows the morphology of electrodeposited nickel and Ni/CeO_2 composite coatings. It can be noticed that the addition of ceria nanoparticles leads to significant changes in coating morphology. Until now, three mechanisms have been proposed for co-deposition: electrophoresis, mechanical entrapment, and particle adsorbtion onto cathode surface by van der Waals interactions.[7] During electrodeposition, hydrogen and nickel hydroxide are formed and partially adsorb onto cathode surface. Moreover, nickel ions also adsorb on the surface of ceria particles; thus, they are attracted to the growth centers on the cathode hindering the grain growth.[8]

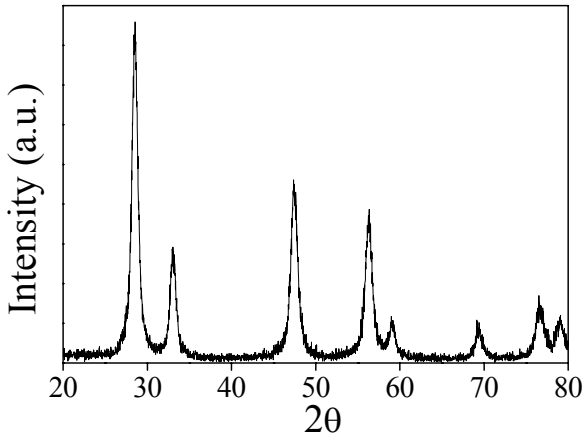

Fig. 1 – XRD pattern of ceria calcined powder.

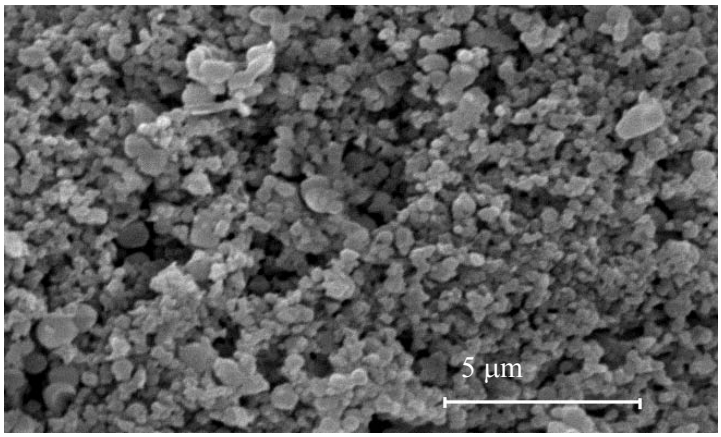

Fig. 2 – SEM image of calcined ceria powder.

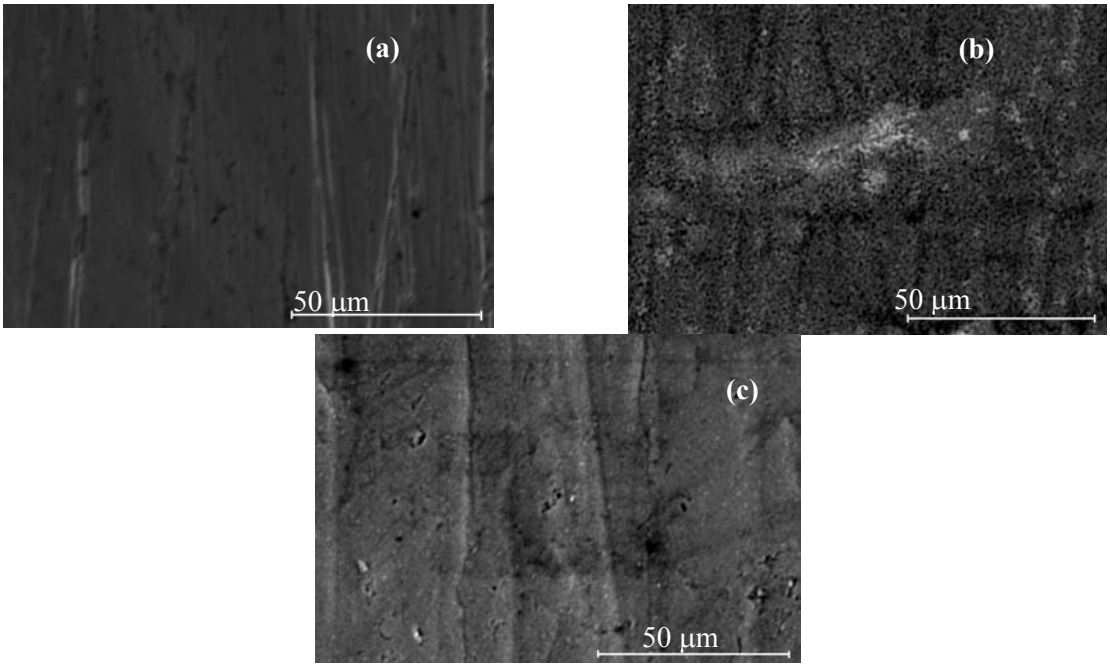

Fig. 3 – SEM images of: (a) carbon steel substrate; (b) Ni coating; (c) Ni/CeO_2 composite coating.

Corrosion behavior in 0.1M HCl

The anticorrosive properties of Ni and Ni/CeO_2 composite coatings in 0.1M HCl solution were investigated by potentiodynamic polarization and impedance spectroscopy.

Potentiodynamic curves

The potentiodynamic curves obtained after 30 min of immersion are presented in Fig. 4.

It can be noticed that the insertion of CeO_2 oxide into nickel matrix leads to a shift of corrosion potential towards more negative values. The presence of CeO_2 oxide does not disturb significantly the anodic reaction but affects the hydrogen evolution. Nevertheless, a decrease of the anodic and cathodic overvoltage was evidenced, mainly due to the parallel displacement towards more negative values.

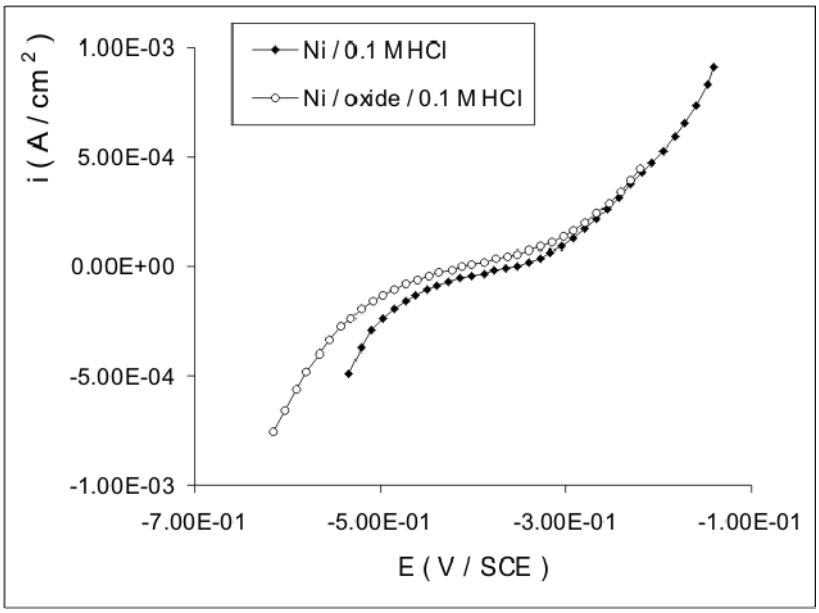

Fig. 4 – Potentiodynamic curves obtained for Ni coating and Ni/CeO_2 composite coating after potential sweep in 0.1 M HCl solution.

Tafel polarization

In Tafel domain, the polarisation curves were registered in the potential range (-700) – (-100) mV with respect to E_{OCP}, with a scan rate of 1 mV/s. Tafel diagram obtained after 30 min of immersion are presented in Fig. 5. The extrapolation of anodic and cathodic Tafel lines of charge transfer controlled corrosion reaction gives the corrosion current density, i_{corr}, at the corrosion potential, *Ecorr*.

The corrosion current was calculated at intercept of the anodic and cathodic Tafel lines, resolving the system of equations listed in Fig. 5.[9, 10]

A decrease of corrosion current density ($i_{corr.}$) in the presence of CeO_2 was evidenced, indicating a more efficient protective action of Ni/CeO_2 composite coating on carbon steel surface than the pure Ni coating. The anodic and cathodic Tafel slopes (b_a & b_c) were slightly modified by the presence of CeO_2 (see Table 1). This behavior can be ascribed to the surface blockage by the oxide. Thus, the anodic dissolution and cathodic hydrogen evolution reaction were both inhibited by CeO_2 through the blockage of the reaction sites on the carbon steel surface, without affecting the anodic and cathodic reaction mechanism.

The protection efficiency (P %) was also evaluated from the polarization data using the following equation:

$$p = \frac{i'_{corr} - i_{corr}}{i'_{corr}} \times 100 \quad (1)$$

where i'_{corr} and i_{corr} are the corrosion current densities in absence and in presence of CeO_2.

It can be noticed that the protection efficiency in the presence of 0.1 g CeO_2 oxide exceeds 46.8 %, which implies a higher corrosion resistance. This behavior can be attributed to the more compact morphology of protective layer when ceria particles are inserted into nickel matrix. It can be assumed that composite layer has a relative uniformity, is adherent, compact and modifies the electronic transfer at the interface.

Polarization resistance technique

The polarization curves obtained in the potential ranges near to corrosion potentials were recorded with a scan rate of 1 mV/s. The linearization was accomplished in the overvoltage range ± 10 mV with respect to E_{corr} (Fig. 6).

The line slopes $(di/dE)_{E \to Ecorr}$ from Fig. 6 represent the polarization conductance. Polarization resistance (R_p, Ω cm^2) was calculated using equation (2):

$$\left(\frac{di}{dE}\right)_{E \to E_{corr}} = \frac{1}{R_p} \quad (2)$$

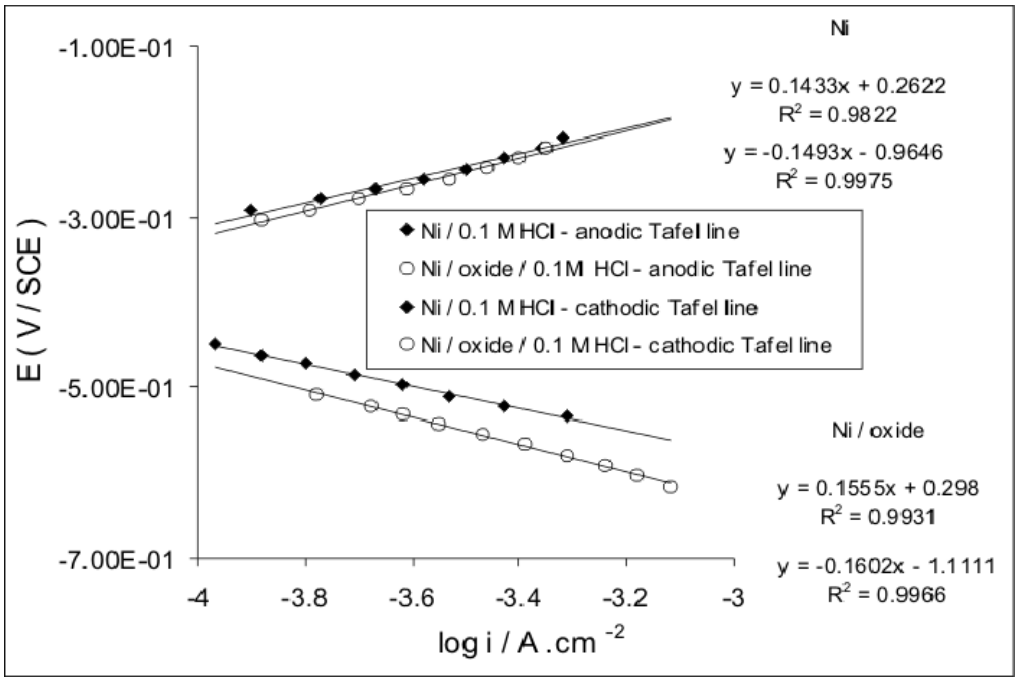

Fig. 5 – Tafel plots for Ni coating and Ni/CeO_2 composite coating after potential sweep in 0.1 M HCl solution.

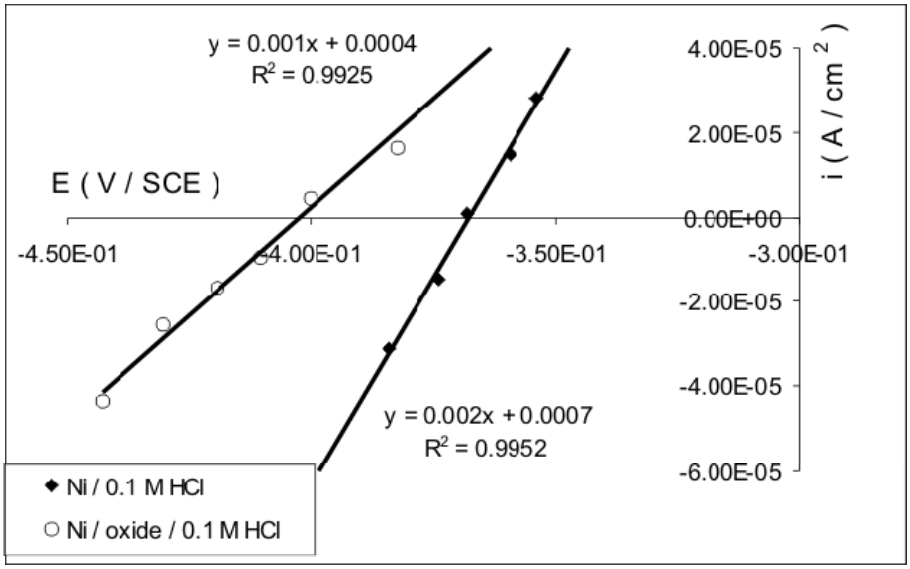

Fig. 6 – Polarization resistance (R_p) diagram of Ni coating and Ni/CeO_2 composite coating obtained after potential scan in 0.1 M HCl solution.

The investigation of the polarization response for Ni and composite coatings in 0.1 M HCl solution shown a shift of polarization resistance (R_p) to a higher value in presence of CeO_2 (Fig. 6 and Table 1). The presence of CeO_2 significantly change the texture of Ni coating, resulting in the formation of impermeable layer, in good agreement with SEM images (Fig. 2). This layer restrains faradaic processes such as electrode oxidation and the exchange of electrons between the electrode and solution. The property of this blockage is attributed to the compactly packed structure of the layer, which obstructs the approach of Cl^- ions from solution to the electrode surface.

The protection efficiency (P %) of Ni/CeO_2 composite coating was calculated according to the following equation:

$$P = \left(1 - \frac{R_p^0}{R_p}\right) \times 100 \quad (3)$$

where R^0_p is polarization resistance in absence of oxide and R_p is the polarization resistance in presence of oxide. .

The protection efficiency and the numerical values of the electrochemical parameters regarding the behavior of Ni coating and Ni/CeO_2 composite coating after corrosion in 0.1 M HCl solution, at room temperature are listed in Table 1.

Table 1

The effect of CeO_2 on the corrosion potential ($E_{corr.}$), corrosion current density ($i_{corr.}$), Tafel slopes (b_a & b_c), protection efficiency (P %) of Ni coating corroded in 0.1 M HCl solution, at room temperature

Coating	E_{corr} (mV / SCE)	i_{corr} (μA cm^{-2})	R_p (Ω. cm^{-2})	b_a mV dec^{-1}	b_c mV dec^{-1}	P(%)	
						from Tafel	from R_p
Ni	-365	64	500	143	149	0	0
Ni / CeO_2	-411	34	1000	155	160	46.8	50

Electrochemical impedance measurements for all investigated samples in 0.1 M HCl solution were carried out at the open circuit potential, after immersion time of: 30 minutes, 3 days; 5 days; 7 days, in the frequency range from 2.10^5 to 10^{-1} Hz, with a value of 10 mV for the amplitude. In Fig. 7 Nyquist plots of impedance spectra of investigated coatings in 0.1 M HCl, at room temperature are shown. One capacitive loop can be observed in Nyquist plots of impedance spectra. More pronounced capacitive loops were obtained for the samples coated with the composite layer. Moreover, a shift towards lower frequency of this contribution when ceria oxide was incorporated into Ni matrix can be noticed. This behavior is usually assigned to changes in density and

composition of substrate coating. Furthermore, the Nyquist plots are not perfect semicircles in the investigated frequency range. This difference is characteristic for solid electrodes and usually referred to as frequency dispersion which has been attributed to roughness and other inhomogeneities of solid electrode surface.

The results show that R_p increases in time. This behavior is more pronounced in the case of composite coating, suggesting an increase in protection efficiency of composite layer compared to the pure Ni coating.

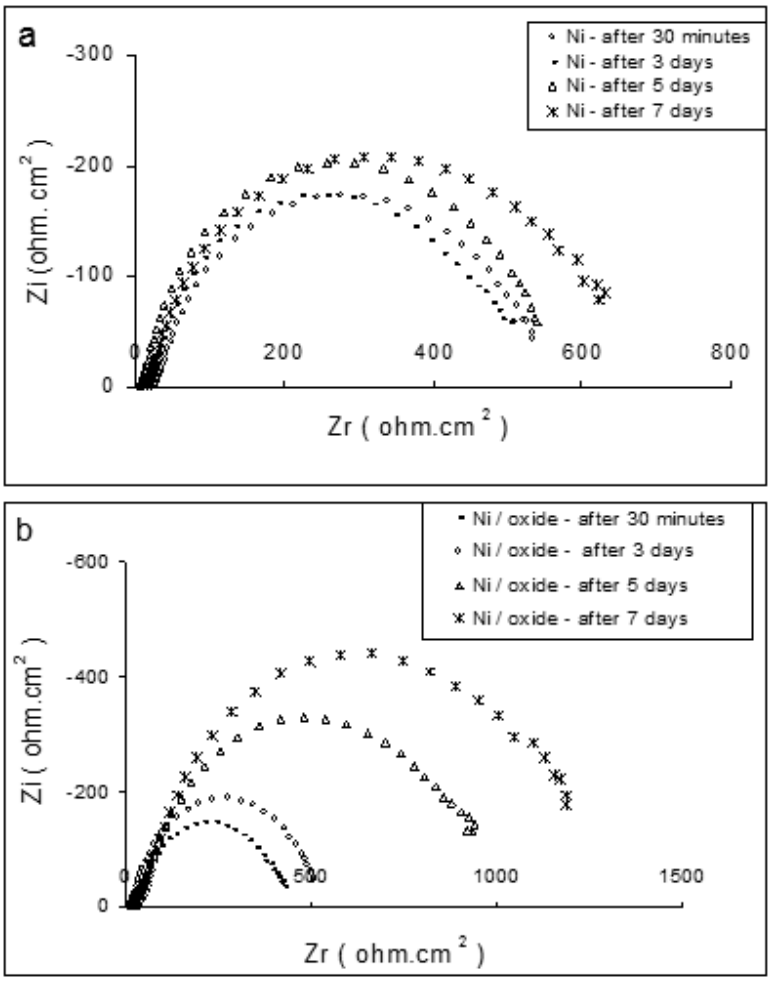

Fig. 7 – Nyquist plots of impedance spectra recorded in 0.1M HCl after different imersion periodes for: (a) Ni coating; (b) Ni/CeO_2 composite coating.

EXPERIMENTAL

Ceria powder synthesis and characterization

Nanostructured ceria powder has been synthesized from cerium nitrate hexahydrate via a modified Pechini method which involves the metal cation chelation with citric acid (in a molar ratio citric acid/total metal = 4.5), followed by polyesterification with ethylene-glycol (using a molar ratio citric acid/ethylene-glycol = 2). In this respect, the nitrate was dissolved in distilled water to obtain an 0.4 M aqueous solution. 8 % vol Triton X-100 was used as structure-directing agent. Subsequently, citric acid was added and the mixture was heated at 80 ºC under reflux and vigurous stiring for 2 h to ensure the complete dissolution of precursor. The polyesterification reaction was initiated by adding ethylene-glycol in the reaction mixture. After heating for 3 h, the excess water was removed with a rotary evaporator, leading to a gel. Finally, the gel was dried in air for 12 h and the resulted solid resin was calcined in air at 550 ºC for 6 h.

The crystallinity of the powder was identified by X-ray diffraction using a D8 Bruker diffractometer equipped with Vantec1 linear detector. The analysis of powders was performed in the 2θ range of 20-75° with a 0.0148° step size. A Jeol 5300 scanning electron microscope (SEM) was used to reveal the powder morphology.

Electrodeposition of Ni and Ni/CeO_2 coatings

For nickel electroplating, a bath with the following composition was used: 300 g/L $NiSO_4 \cdot 7H_2O$, 60 g/L $NiCl_2 \cdot 6H_2O$, 30 g/L H_3BO_3. The bath temperature was kept at

25 ± 1°C. For electrodeposition of Ni-ceria composite, nanostructured CeO_2 powder (2 g/L) was added to the electrolyte. To ensure a uniform dispersion of particles, the electrolyte was stirred for 2 h before the deposition. A platinum plate with dimensions 35 mm × 10 mm × 1 mm was used as the anode, and a carbon steel plate with dimensions 10 mm × 10 mm × 1 mm was used as cathode. The carbon steel composition was: 0.045 wt % C, 0.037 wt % Si, 0.21 wt % Mn, 0.012 wt % Mn, 0.018 wt % S, 0.045 wt % Al, and 99.624 % wt Fe. The polished carbon steel substrate was degreased with acetone and washed with distilled water. The electrodeposition was carried out with a Solartron 1280B Potentiostat/Galvanostat. The electrolyte bath was magnetically stirred (300 rpm) during electrodeposition process. The deposition was carried out at 3 A/dm^2 for 1 h.

The morphology of electrodeposited coatings was evidenced with a Jeol 5300 scanning electron microscope.

Corrosion behavior in 0.1 M HCl solution

Electrochemical investigation of Ni and Ni/CeO_2 coated samples were performed with a Solartron 1280B Potentiostat/Galvanostat with built-in frequency response analyzer. The surface area exposed to the corrosive medium was 1 cm^2. A platinum foil with 1 cm^2 area was used as counter electrode, and saturated calomel electrode was used as reference electrode. The measurements were carried out in free air 0.1 M HCl aqueous solution. The investigated sample was imersed into HCl solution for 30 min in order to attain the open circuit potential (E_{OCP}). The impedance spectra were recorded at open circuit potential, in the frequency range 20 kHz - 0.1Hz with a signal amplitude of 10 mV. The system was then allowed to attain the open circuit potential and the potentiodynamic polarization measurements were carried out in the range of ± 200 mV with respect to E_{OCP}. The rate of potential change was set at 1 mV/s. The Tafel plots were thus obtained.

CONCLUSIONS

Nanostructured ceria have been synthesized by a modified Pechini method, using Triton X-100 as structure-directing agent. Compact Ni/CeO_2 layer have been obtained by electrochemical deposition from a Watt bath with nanosized ceria addition. Insertion of ceria nanoparticles into nickel matrix lead to an improvement of electrodeposited layer morphology. Corrosion behavior of pure Ni and Ni/CeO_2 composite coatings in 0.1M HCl solution was investigated. An increase in protective efficiency was obtained after insertion of ceria nanoparticles into nickel matrix. Moreover, electrochemical impedance spectroscopy measurements revealed an increase in polarization resistances in time. Higher values of polarization resistance were obtained for composite layer after 5 and 7 days, respectively, as compared to pure Ni coating.

Acknowledgements: Financial support from the POSDRU/6/1.5/S/14 Project "Increasing attractivity, quality and efficiency of doctoral university studies confering doctoral scholarships" is gratefully acknowledged.

REFERENCES

1. A.E. Hughes, R.J. Taylor, B.R.W. Hinton and L. Wilson, *Surf. Interface Anal.*, **1995**, *23*, 540-550.
2. S. Roure, F. Czerwinski and A. Petric, *Oxid. Met.*, **1994**, *42*, 75-102.
3. I. Zhitomirsky and A. Petric, *Ceram. Int.*, **2001**, *27*, 149-155.
4. I. Shao, P.M. Vereecken, C.L. Chien, P.C. Searson and R.C. Cammarata, *J. Mater. Res.*, **2002**, *17* 1412-1418.
5. I. Shao, P.M. Vereecken, R.C. Cammarata and P.C. Searson, *J. Electrochem. Soc.*, **2002**, *149*, 610-614.
6. B. Szczygieł and M. Kołodziej, *Electrochim. Acta*, **2005**, *50*, 4188-4195.
7. C. Buelens, J. Fransaer, J.P. Celis and J.R. Roos, *Bull. Electrochem.*, **1992**, *8*, 371-377.
8. N.S. Qu, D. Zhu and K.C. Chan, *Scripta Materialia*, **2006**, *54*, 1421-1425.
9. A. Samide and I. Bibicu, *Rev. Roum. Chim.*, **2009**, *54*, 33-43.
10. A. Samide, I. Bibicu, M. Floroiu, M. Preda and B. Tutunaru, *Rev. Roum. Chim.*, **2007**, *52*, 569-576.